

## DEFECT ANALYSIS OF APCVD GETTERED MULTICRYSTALLINE SILICON

Martin Fleck, Jeanette Lindroos, Annika Zuschlag, Giso Hahn  
 University of Konstanz, Department of Physics, 78457 Konstanz, Germany  
 martin.fleck@uni-konstanz.de, Tel: +49 7531 882082, Fax: +49 7531 883895

**ABSTRACT:** The effects of atmospheric pressure chemical vapor deposition (APCVD) gettering on material quality of industry standard mc-Si wafers has been studied on a microscopic level and compared to  $\text{POCl}_3$  gettering samples. The interaction of the gettering efficacy with the microscopic defect structure has been studied by a combination of measurements of the effective minority charge carrier lifetime ( $\tau_{\text{eff}}$ ), interstitial iron ( $\text{Fe}_i$ ), optical microscope images of defect structures revealed with Secco etching, a subsequent high resolution etch pit density (EPD) analysis as well as Electron Beam Induced Current (EBIC) and Electron Backscatter Diffraction (EBSD). Findings include a similar gettering quality of APCVD- and  $\text{POCl}_3$ -based glasses and a reduction of EPD after the gettering step.

**Keywords:** Multicrystalline Silicon, Gettering, APCVD, Lifetime, Defects

## 1 INTRODUCTION

Gettering is known to strongly increase material quality of multicrystalline silicon. With APCVD (atmospheric pressure chemical vapor deposition)-based glasses, doping sources and getter sinks can easily and cost effectively deposited on one side only, making this technology valuable for passivated emitter, rear totally diffused (PERT) and other advanced solar cell concepts. Here we make a comparison between APCVD and  $\text{POCl}_3$  based gettering and the interaction of the gettering efficacy with the microscopic defect structure, for which measurements of effective minority charge carrier lifetime ( $\tau_{\text{eff}}$ ), interstitial iron concentration ( $[\text{Fe}_i]$ ), optical microscope images of Secco etched wafers, etch pit density (EPD), electron beam induced current (EBIC) and electron backscatter diffraction (EBSD) are combined.

## 2 EXPERIMENTAL

### 2.1 Sample Processing

Industrial multicrystalline silicon sister wafers with boron doped bulk and a resistivity of  $1 \Omega\text{cm}$  from middle ingot height were, after typical saw damage removal and cleaning steps, subjected to either of the following (Fig. 1): Either an APCVD BSG (boron-silicate glass) and PSG (phosphosilicate glass) deposition followed by a high temperature diffusion step at  $840^\circ\text{C}$  (referred to as APCVD gettering in the following) or else solely the previously mentioned high temperature step at  $840^\circ\text{C}$  or an industry standard  $\text{POCl}_3$  diffusion. Hereafter, emitter and BSF (back surface field) were removed followed by PECVD (plasma-enhance chemical vapor deposition) deposition of  $\text{SiN}_x\text{:H}$  and firing.

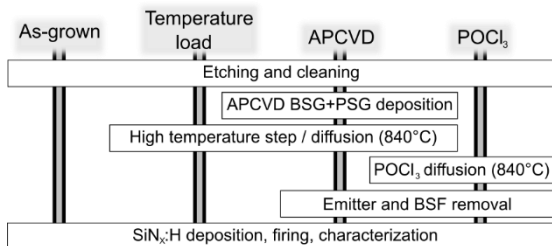


**Figure 1:** Process flow that the various samples have been subjected to.

### 2.2 Etching and etch pit density counting algorithm

Etch pits were formed by application of the Secco etch [1] on mechanically polished wafers for an etching time of 180 s. During the etching process, the beaker was agitated in an ultrasonic bath.

The etched wafer surface is recorded with an optical microscope. The etch pit density counting algorithm is based on [2]. The outline of the algorithm that was used is roughly as follows:

1. Thresholding of the image (black and white conversion)
2. Removal of small specks
3. Identification and characterization of remaining structures
4. Separation of the largest structure(s)
5. Counting of small structures – these are free standing, individual etch pits
6. Distinguishing between grain boundaries and high density clusters of etch pits
7. Estimation of the density of etch pits in regions where the etch pits are so dense that they cluster together to a compound structure (etch pit cluster). Based on the size distribution of the free standing etch pits of the current sample, an estimator for the density of etch pits in such clustered regions is calculated.
8. Filling of thus acquired spatial information of free standing and clustered etch pits into a single histogram results in the EPD maps as shown in this publication

The algorithm outlined above will be discussed and in detail and released in a future publication.

## 3 RESULTS

On the macroscopic scale, effective minority carrier lifetime ( $\tau_{\text{eff}}$ ) and interstitial iron ( $\text{Fe}_i$ ) maps are accessible via QSSPC (quasi-steady-state photoconductance) calibrated photoluminescence (PL) imaging. The PL and  $\text{Fe}_i$  images shown in Fig. 2 and Fig. 3 are a superposition of the optical image of the Secco etched wafer with the respective map of the measurement variable, either  $\tau_{\text{eff}}$  or  $[\text{Fe}_i]$ . Hence, defects revealed by the Secco etch are visible as black structures on top of the map.

### 3.1 $\tau_{\text{eff}}$ and $[\text{Fe}_i]$ correlation

Macroscopic measurement variables for gettering strength used in this study are  $\tau_{\text{eff}}$  and  $[\text{Fe}_i]$  (Fig. 2, Fig. 3). Temperature treatment slightly, if at all, decreases the harmonic mean of  $\tau_{\text{eff}}$  from 60  $\mu\text{s}$  in the as-grown state to 59  $\mu\text{s}$  in accordance with the slight increase in  $[\text{Fe}_i]$ . APCVD ( $\text{POCl}_3$ ) based gettering results in mean values for  $\tau_{\text{eff}}$  of 158  $\mu\text{s}$  (170  $\mu\text{s}$ ), respectively. Comparably strong gettering effects are observed for APCVD and  $\text{POCl}_3$  getterted samples as already described in [3]. The observed increase in  $\tau_{\text{eff}}$  (Fig. 2) is similar for both gettering methods whereas the reduction in interstitial iron in the depicted sample is stronger for the APCVD getterted sample. However, it should be noted that the comparison of  $\tau_{\text{eff}}$  and  $[\text{Fe}_i]$  (Fig. 3) for various column heights and block positions is sometimes in favor of APCVD and sometimes in favor of  $\text{POCl}_3$  getterting. Therefore, no clear tendency can be detected.

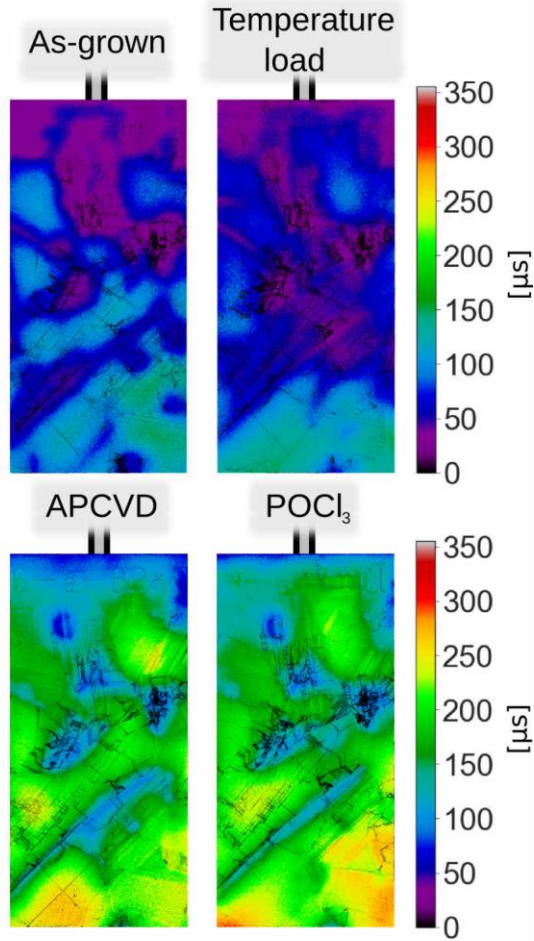


**Figure 2:**  $\tau_{\text{eff}}$  maps of as-grown, temperature treated (840°C), and APCVD as well as  $\text{POCl}_3$  getterted samples. Sample size: 12x25 mm<sup>2</sup>.

When isolating the temperature load of the diffusion step (840°C) in absence of an external getter sink, a redistribution of  $\text{Fe}_i$  is observed, *i.e.* a slight overall increase in the as-grown  $[\text{Fe}_i]$  in regions of low and intermediate contamination strength, combined with a decrease in size of highly contaminated regions. Consequently, a slight reduction of  $\tau_{\text{eff}}$  is observed. In

absence of an external getter sink, no effective gettering effect is observed.

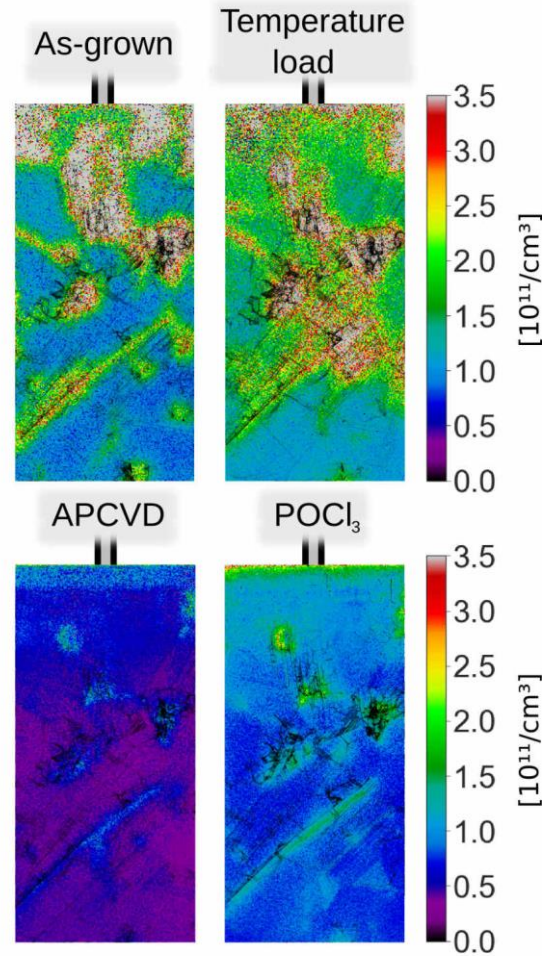


**Figure 3:**  $[\text{Fe}_i]$  maps of as-grown, temperature treated (840°C), and APCVD as well as  $\text{POCl}_3$  getterted samples. Sample size: 12x25 mm<sup>2</sup>.

A clear correlation between  $\tau_{\text{eff}}$  and  $[\text{Fe}_i]$  is observed on the scale of millimeter sized structures within each of the differently treated samples. Regions of high  $\text{Fe}_i$  typically perform poor in  $\tau_{\text{eff}}$  and *vice versa*.

Gettering is most effective, *i.e.* relative improvements are strongest, in regions of high  $[\text{Fe}_i]$ . This suggests the interpretation that the prepared gettering conditions (getter sink properties and temperature) are capable of reducing the contamination to a certain value, despite the presence of defect clusters that are typically found in high  $[\text{Fe}_i]$  regions (Fig. 3).

### 3.2 Extended crystal defect density

The EPD of the as-grown sample reveals a clear correlation between high  $[\text{Fe}_i]$  and high EPD (Fig. 4).

The sample set presented here shows considerable EPD reduction for the  $\text{POCl}_3$  getterted sample (Fig. 4) and only very slight EPD reduction after APCVD getterting. Additional sample sets from different ingot heights and positions have shown an APCVD EPD reduction that is relatively stronger than for its sister  $\text{POCl}_3$  getterted

sample while at the same time exhibiting an absolute EPD reduction comparable to the  $\text{POCl}_3$  sample depicted here. There is currently no indication for a correlation between the strength of EPD reduction and  $[\text{Fe}_i]$  results.

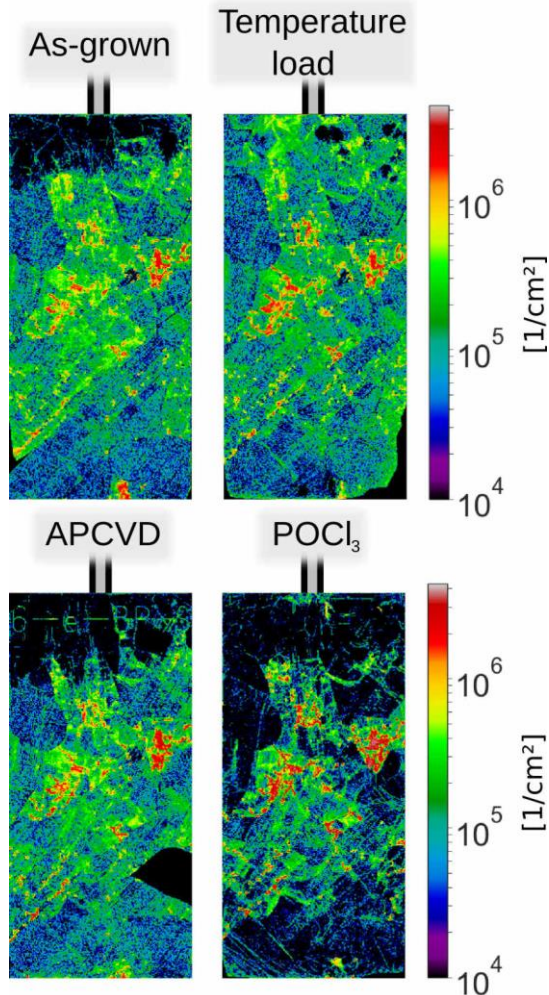


**Figure 4:** EPD maps of as-grown, temperature treated (840°C), and APCVD as well as  $\text{POCl}_3$  gettered samples. The top region of these samples was influenced by the carrier that was used during the Secco etch and should thus be ignored. Sample size: 12x25 mm<sup>2</sup>.

Temperature load in absence of a getter sink has in some samples shown a slight EPD reduction (not the case for the sample shown here). The applied temperature of 840°C should normally not result in movement/annihilation of dislocations which usually takes place at significantly higher temperatures only. Nevertheless, similar effects have been observed before [4] and the underlying mechanism is still unclear. Further investigations are ongoing.

### 3.3 Recombination activity

EBIC measurements offer a unique possibility to analyze spatially resolved recombination activity with a similar high resolution as the microscopic etch pit density analysis.

The EBIC measurement of the temperature load sample (Fig. 5) features a more homogeneous EBIC

contrast in comparison to the as-grown sample: Clouds of higher recombination activity in the vicinity of the most dense regions of recombination active defect lines and grain boundaries are not visible or less pronounced in the temperature load sample.

The comparison of EBIC signals of the as-grown and APCVD gettered samples with the corresponding EBSD map of the APCVD gettered sample (Fig. 6) reveals that most of the recombination active structures remaining after gettering are defect lines. Most grain boundaries show negligible recombination activity after gettering for both gettering methods. Only small parts of a few grain boundaries retain their recombination activity. This was observed for large angle as well as small angle grain boundaries.

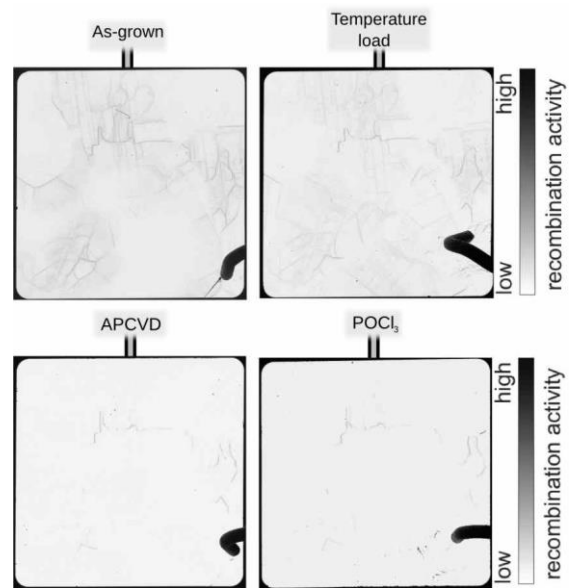


**Figure 5:** EBIC maps of as-grown, temperature treated (840°C), and APCVD as well as  $\text{POCl}_3$  gettered samples revealing the recombination activity close to the sample surface. Sample size: 9x9 mm<sup>2</sup>, taken roughly from the middle of the samples depicted in Figs. 2-4.

APCVD as well as  $\text{POCl}_3$  gettered samples show strongly reduced recombination activity and feature very few remaining recombination active structures. Remaining structures consist mostly of defect lines. Only few of the remaining structures are grain boundaries.

## 5 CONCLUSION

Similarly strong effects for APCVD and  $\text{POCl}_3$  based gettering were observed. Gettering is most effective in high  $[\text{Fe}_i]$  regions, despite high EPD in these areas. All samples show a strong correlation in local structures of  $\tau_{\text{eff}}$  and  $[\text{Fe}_i]$  maps.

The gettering step introduces a reduction of EPD for APCVD as well as  $\text{POCl}_3$  based gettering. Furthermore, APCVD and  $\text{POCl}_3$  based gettering result in strong improvement of the EBIC signal. Recombination active structures that remain after the gettering steps are some defect lines as well as (segments of) large and small angle grain boundaries.



**Figure 6:** Comparison of EBIC results for the as-grown (top) and APCVD gettered sample (middle) with the misorientation angle between grains at grain boundaries measured via EBSD. The APCVD gettered sample was used for the EBSD measurement.

## 6 ACKNOWLEDGEMENTS

Part of this work was supported by the German Federal Ministry of Economic Affairs and Energy under contract no. 0324041B and 0324001. The content is the responsibility of the authors.

## 7 REFERENCES

- [1] F. Secco d' Aragona, *Journal of the Electrochemical Society* 119(7) 1972-948.
- [2] D.B. Needleman, H. Choi, D.M. Powell, T. Buonassisi, *Physica Status Solidi Rapid Research Letters* 7(12) (2013) 1041.
- [3] D.P. Fenning, A.S. Zuschlag, J. Hofstetter, A. Frey, M.I. Bertoni, G. Hahn, T. Buonassisi, *IEEE Journal of Photovoltaics* 4(3) 866.
- [4] J. Fichtner, H. Zunft, A. Zuschlag, H. Knauss, G. Hahn, *IEEE Journal of Photovoltaics* (2018) in press; DOI: 10.1109/JPHOTOV.2018.2865509